Neural Block Controller with Input Constrains for Induction Motors

Ramon A. Felix, Edgar N. Sanchez and Alexander G. Loukianov.
CINVESTAV, Unidad Guadalajara, Apartado Postal 31-438, Plaza La Luna, Guadalajara, Jalisco, C.P. 45091, Mexico, e-mail:rfelix@gdl.cinvestav.mx

Abstract— **In this paper we present a novel approach to control induction motor, considering the switching nature of their electrical drivers. Modifying published results for nonlinear identification using dynamic neural networks, we propose a neural network identifier. The controller is derived using the neural block control technique and sliding modes control. Such control law is a discontinuous one, which just takes values from the look-up table given by the inverter circuit connected to the stator windings, This control strategy is motivated by the wearing that suffer the switching electronic devices, when a PMW approach is used at high frequency operation.**

Keywords— **Induction Motors, Variable Stucture Control, Hybrid Systems, Electrical Drivers, Neural Networks.**

I. Introduction

For electrical motors applications the drives are basically constant voltage sources connected to the motor windings by power electronic switching devices (BJT, GTO, IGBT, etc.). In these cases, frequently the PWM (Pulse Width Modulator)[7] is used to approach the desired control signal. Such modulator forces each power device to switch on and off, for each sample time. However, if the devices are operated at high frequency, this switching PWM strategy may destroy the electronic devices in a short time period, since for every switching (on and off) there is a dissipated power peak.

Induction motors are widely used in industrial applications due to their reliability, simpler construction and reduced cost with respect, for example, to d.c. motors. However, the control of induction motors is a difficult problem due to their highly nonlinear dynamics [7]. For the design control procedure, it is important however to take into account the discrete feature of the electrical drives, as done in [3], where the Direct Torque Control (DTC), a heuristic control strategy for high power induction motor application, is proposed. As well as our approach, it switches the power devices just one time, for each sample time. The DTC is particularly appealing for slow-sampling applications, where the average approximation used for the implementation of modulation-based control may be inadequated. There has been some efforts to study the DTC controller stability, for example [11] and [2].

In this paper, based on the Variable Structure Control (VSC) method [16], we propose a discontinuous control strategy for induction motors. Such control scheme enables to reduce the device switching to only one during the sample time, instead of the two switching required by the PWM. This enables to reduce the power electronic devices wearing, and increase theirs life span. Additionally, this approach is robust against external disturbances fulfilling the matching condition.

Modifying existing identification schemes based on dynamic neural networks [6], a neural network identifier of block controllable form is proposed. Based on VSC and Block Control [8], we propose a hybrid control law, which consists of switching the inverter power devices. This strategy guarantees a stable sliding mode motion on the desired nonlinear manifold, where the rotor speed and flux tracking errors tend to zero. The main contribution of this work is to trade off between technological constraints and stability analysis

II. Induction Motor Model

For electrical motors applications, the drives are basically constant voltage sources connected to the motor windings by power electronic switching devices (BJT, GTO, IGBT, etc.). Fig. 1 shows a switched inverter, connected to a three-phase induction motor [7]. The switching elements may be, for example, IGBT(Insulated-Gate Bipolar Transistor). Each IGBT pair can be manipulated by one of the control binary variables a, b and c. The power transistors are commuted from the ON (saturation) to the OFF(cut-off) state and vice versa, depending on theirs corresponding binary variables, as illustrated in Fig. 1. All binary variables may change their states independently. Hence, there are eight possible combinations.

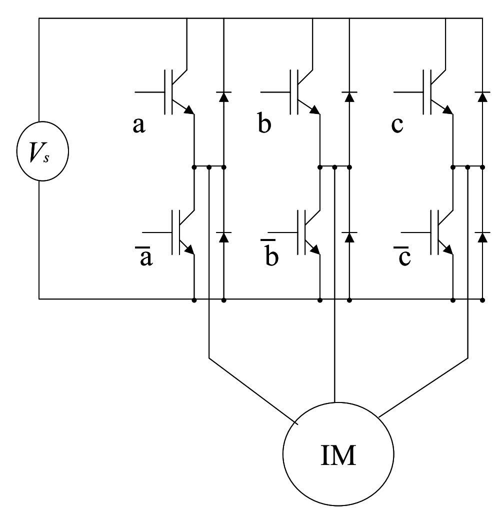

Fig. 1. The inverter and induction motor connection.

A three-phase circuit can be reduced to a more convenient two-phase model. Let define the input voltage vector $\mathbf{u} = [u_\alpha \ u_\beta]^\top$, in the two-phase $\alpha - \beta$ reference frame [1], where u_α and u_β stand, respectively, for the voltage applied to the induction motor stator windings. Then, the available input vectors are restricted to a discrete set U. The relation between these voltages vectors and the binary variables (a, b and c) is formulated as

abc	U	u_α	u_β
000	$\mathbf{u_0}$	0	0
100	$\mathbf{u_1}$	$2V_s/3$	0
110	$\mathbf{u_2}$	$V_s/3$	$V_s/\sqrt{3}$
010	$\mathbf{u_3}$	$-V_s/3$	$V_s/\sqrt{3}$
011	$\mathbf{u_4}$	$-2V_s/3$	0
001	$\mathbf{u_5}$	$-V_s/3$	$-V_s/\sqrt{3}$
101	$\mathbf{u_6}$	$V_s/3$	$-V_s/\sqrt{3}$
111	$\mathbf{u_7}$	0	0

Table 1. Binary variables and theirs corresponding input voltages vectors

where V_s is given by the constant voltage source, which feeds the inverter. Figure 2 is the phase portrait of the available input vectors.

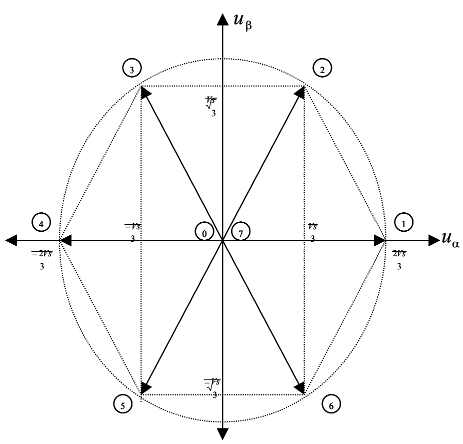

Fig. 2. Avaliable Stator Voltages Vectors

In many applications the discrete constrains (Table 1) imposed by the inverter (Figure 1) are solved by using a PWM (Pulse Width Modulator) approach [7]. So one may suppose that input $\mathbf{u}$ can be any bounded time function. The control law in derived considering such constrains.

The following set equations are presented in the stator-fixed $\alpha-\ \beta$ coordinate system (see for instance [1]), they describes the induction motor dynamics

$$\begin{aligned}
\dot{\chi}_1 &= c_1(\chi_2\chi_5 - \chi_3\chi_4) - c_0 T_L \\
\dot{\chi}_2 &= -c_2\chi_2 - n_p\chi_1\chi_3 + c_3\chi_4 \\
\dot{\chi}_3 &= -c_2\chi_3 + n_p\chi_1\chi_2 + c_3\chi_5 \qquad (1)\\
\dot{\chi}_5 &= c_4\chi_2 + c_5 n_p\chi_1\chi_3 - c_6\chi_4 + c_7 u_\alpha \\
\dot{\chi}_6 &= c_4\chi_3 - c_5 n_p\chi_1\chi_2 - c_6\chi_5 + c_7 u_\beta
\end{aligned}$$

where χ_1 represents the angular velocity of the motor shaft, χ_2 and χ_3 are, respectively, the rotor magnetic flux leakage components, χ_4 and χ_5 are, respectively, the stator current components, u_α and u_β stand, respectively, for the voltage applied on the stator windings, and T_L represents the load torque perturbation. The constants c_i, $i = 0, ..., 7$ are defined as follows:$c_0 = \frac{1}{J}$, $c_1 = \frac{3}{2}\frac{M n_p}{J L_r}$, $c_2 = \frac{R_r}{L_r}$, $c_3 = \frac{R_r M}{L_r}$, $c_4 = \frac{R_r}{L_r}\frac{M}{L_s L_r - M^2}$, $c_5 = \frac{M}{L_s L_r - M^2}$, $c_6 = \frac{R_s L_r^2 + R_r M^2}{L_s(L_s L_r - M^2)}$, $c_7 = \frac{L_r}{L_s L_r - M^2}$

with L_s, L_r and M, respectively, being the stator and rotor inductances and mutual inductance between the rotor and the stator, R_s and R_r, the stator and rotor resistances, J the rotor moment of inertia and n_p the number of stator winding pole pairs.

Commonly, induction motor applications require not only the shaft speed regulation, but also the flux magnitude $\phi = \chi_2^2 + \chi_3^2$ regulation. Based on this model, the so-called dynamic block controllable neural network is proposed.

III. Nonlinear observer

ince the currents and velocity are the only measurable variables the rotor fluxes estimation is required for neural networks identification. This flux estimator was proposed in [9]; it is a partial state observer with adjustable convergence rate. This features enables to reduce the number of calculations comparing with a full state observer. To obtain the flux estimation, only the stator currents dynamics is used. The proposed observer has the following form

$$\begin{aligned}
\dot{\tilde{\chi}}_4 &= -c_5\chi_4 + c_6 u_1 + v_\alpha \\
\dot{\tilde{\chi}}_5 &= -c_5\chi_5 + c_6 u_2 + v_\beta
\end{aligned}$$

where $\tilde{\chi}_4$ and $\tilde{\chi}_5$ are the estimation of currents χ_4 and χ_5 and $\mathbf{v} = [\mathbf{v_\alpha} \ v_\beta]^\top$is the observer input.

Let define current observer error as $\varepsilon_\alpha = \chi_4 - \tilde{\chi}_4$ and $\varepsilon_\beta = \chi_5 - \tilde{\chi}_5$, whose dynamics is given by

$$\begin{aligned}
\dot{\varepsilon}_\alpha &= c_4\chi_2 + c_5 n_p\chi_1\chi_3 - v_\alpha \\
\dot{\varepsilon}_\alpha &= c_4\chi_3 - c_5 n_p\chi_1\chi_2 - v_\beta.
\end{aligned}$$

Then, on the sliding surface ε_α, $\varepsilon_\beta = 0$, the following invariance equation is satistied

$$\begin{aligned}
0 &= c_4\chi_2 + c_5 n_p\chi_1\chi_3 - v_{\alpha eq} \qquad (2)\\
0 &= c_4\chi_3 - c_5 n_p\chi_1\chi_2 - v_{\beta eq}
\end{aligned}$$

with $\mathbf{v_{eq}} = [\mathbf{v_{\alpha eq}}, \ v_{\beta eq}]^\top$ as the equivalent value of $\mathbf{v}$.

Now, based on unit control, v_α and v_β are selected as

$$v_\alpha = l_1\frac{\varepsilon_\alpha}{|\varepsilon_\alpha| + \delta} \text{ and } v_\beta = l_2\frac{\varepsilon_\beta}{|\varepsilon_\beta| + \delta}$$

with l_1, l_2 and δ are positive observer parameters.

If l_1, l_2 are enough large and δ is sufficiently small we garantee a sliding motion on surface ε_α, $\varepsilon_\beta = 0$. So $\mathbf{v}$ is taken as an estimated of $\mathbf{v_{eq}}$. Therefore we can express (2) as

$$\begin{bmatrix} c_4 & c_5 n_p\chi_1 \\ -c_5 n_p\chi_1 & c_4 \end{bmatrix}\begin{bmatrix} \chi_2 \\ \chi_3 \end{bmatrix} = \begin{bmatrix} v_\alpha \\ v_\beta \end{bmatrix}$$

from the this equation, it is possible to obtain the estimation of χ_2 and χ_3 as

$$\begin{bmatrix} \hat{\chi}_2 \\ \hat{\chi}_3 \end{bmatrix} = \frac{1}{c_4^2 + (c_5 n_p \chi_1)^2} \begin{bmatrix} c_4 & -c_5 n_p \chi_1 \\ c_5 n_p \chi_1 & c_4 \end{bmatrix} \begin{bmatrix} v_\alpha \\ v_\beta \end{bmatrix}$$

where the estimated fluxes are $\tilde{\chi}_2$ and $\tilde{\chi}_3$. For the rest of the calculations on this chapter, the estimated fluxes are considered as the real ones.

IV. On-line Identification

Usually, for nonlinear control systems, the plant model is obtained from the plant physics. For neural control, we propose to build a neural model based on a given plant model structure. The RHONN scheme is very flexible and allows to incorporate to the neural identifier a priori information about the plant structure.

Hence, second-order RHONN is used as the identifier [6]. In order to introduce the most possible information about the induction motor and based on the mathematical models for induction motors (1), the following neural model is proposed [9]

$$\begin{aligned} \dot{x}_1 &= -a_1 x_1 + w_{11} S(\chi_1) + w_{12} S(\chi_3)\chi_4 + w_{13} S(\chi_2)\chi_5 \\ \dot{x}_2 &= -a_2 x_2 + w_{21} S(\chi_2) + w_{22} S(\chi_1) S(\chi_3) + w_{23}\chi_4 \\ \dot{x}_3 &= -a_3 x_3 + w_{31} S(\chi_3) + w_{32} S(\chi_1) S(\chi_2) + w_{33}\chi_5 \end{aligned} \quad (3)$$

For this model $\mathbf{w_1} = [w_{11}, w_{12}, w_{13}]^\top$, $\mathbf{w_2} = [w_{21}, w_{22}, w_{23}]^\top$ and $\mathbf{w_3} = [w_{31}, w_{32}, w_{33}]^\top$ are the adaptive RHONN parameters.

with $a_i > 0$, $i = 1, ..., 3$, $w_{i,j}$ are time-varying weights, and $S(\cdot)$ a smooth sigmoid function formulated by:

$$S(x) = \frac{2}{1 + \exp(-\beta x)} - 1$$

for the sigmoid $S(x) \in [-1, 1]$.

For this neural model, x_1 is called neural speed or velocity, and x_2 and x_3 are the neural fluxes, so they are used to identify χ_1, χ_2 and χ_3 respectively.

A. Robust Weight Update Law

In case when the modelling error term is not zero we can not guarantee neither the boundness of the parameters nor the convergence to zero of the identification error. Then we need to apply an adaptive law with the σ-modification [5] in order to guarantee at least, that the identification error and the weights are bounded for any time. Hence we propose the adaptive law

$$\dot{\mathbf{w}}_i = -\Gamma_i^{-1}(e_i \boldsymbol{\rho}_i - \sigma_i \mathbf{w}_i), \quad i = 1, 2, 3 \qquad (4)$$

where σ_i is given as:

$$\sigma_i = \begin{cases} 0, & \text{if } ||\mathbf{w}_i|| \leq M_i \\ \left(\frac{||\mathbf{w}_i||}{M_i}\right)^q \sigma_{i0}, & \text{if } M_i < ||\mathbf{w}_i|| \leq 2M_i \\ \sigma_{i0}, & \text{if } ||\mathbf{w}_i|| > 2M_i \end{cases}$$

with integer $q \geq 1$, and σ_{i_0} and M_i positive constants.

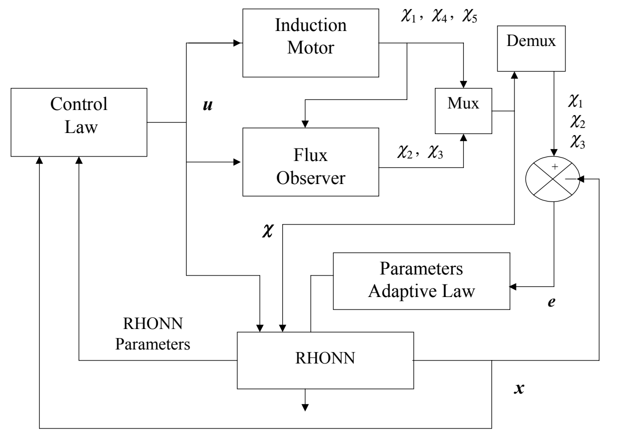

Fig. 3. Block scheme

V. Neural Block Controller

The proposed identification and control scheme Fig. 3 is based on the following proposition

Proposition 1: Given a desired output trajectory, expressed on output variables as $\mathbf{y_r}$, a nonlinear system with output $\mathbf{y_P}$, and a neural network output $\mathbf{y_P}$ then it is possible to establish the inequality

$$\|\mathbf{y_r} - \mathbf{y_P}\|_2 \leq \|\mathbf{y_N} - \mathbf{y_P}\|_2 + \|\mathbf{y_r} - \mathbf{y_N}\|_2$$

where $\|\cdot\|_2$ stands for the Euclidean norm.

Where $\mathbf{y_r} - \mathbf{y_P}$ is called the output system error tracking, $\mathbf{y_N} - \mathbf{y_P}$ the output identification error and $\mathbf{y_N} -$ $\mathbf{y_r}$the output RHONN error tracking. Hence, it is possible to divide the tracking problem in two parts:

a) Minimization of $\|\mathbf{y_N} - \mathbf{y_P}\|_2$,which can be achieved by the proposed on-line identification algorithm.

b) Minimization of $\|\mathbf{y_N} - \mathbf{y_r}\|_2$, for which a tracking algorithm is developed on the basis of the neural identifier (3). The second goal can be reached by designing a control law based on the RHONN model. To design such controller we propose to use the so called Neural Block Control [15], [14]. This control technique requires the plant to have the Block Controllable Form (BCF) [8], so a RHONN identifier with BCF is proposed. Based on this neural model a discontinuous control law, which combines block control [8] and VSC with sliding mode technique [16], is derived. The block control approach is used to design a nonlinear sliding surface such that the resulting sliding mode dynamics is described by a desired linear system.

One additional advantage about using VSC is the separation of the system dynamics in two motions, so that, only a partial state RHONN is needed to derive the control law..

A. VSC Neural Block Controller Design

The output variables to be controlled are the speed χ_1 and the neural flux magnitude ϕ, respectively. Now, let define the neural flux magnitude as $\varphi = x_2^2 + x_3^2$, then, according to Proposition 1 the plant output is $\mathbf{y}_P = [\chi_1 \ \phi]^\top$, the neural output is $\mathbf{y}_N = [x_1 \ \varphi]^\top$ and the reference signal is $\mathbf{y_r} = [\boldsymbol{\omega}_\mathbf{r} \ \varphi_r]^\top$.

The model (3) has a quasi NBC (Nonlinear Block Controllable) form, consisting of two blocks:

$$\begin{aligned}\dot{\mathbf{x}}_1 &= \tilde{\mathbf{f}}_1(\mathbf{x}_1,\boldsymbol{\chi}_1,\mathbf{w})+\tilde{\mathbf{B}}_1(\boldsymbol{\chi}_1,\mathbf{w})\boldsymbol{\chi}_1 \\ \dot{\boldsymbol{\chi}}_2 &= \mathbf{f}_2(\boldsymbol{\chi}_1,\boldsymbol{\chi}_2)+\mathbf{B}_2\mathbf{u} \end{aligned} \tag{5}$$

with $\mathbf{x^1} = [\mathbf{x_1},\mathbf{x_2},\mathbf{x_3}]^\top$, $\boldsymbol{\chi_2} = [\boldsymbol{\chi_4},\boldsymbol{\chi_5}]^\top$, $\mathbf{u} = [u_\alpha,u_\beta]^\top$, $n_1 = 3$ and $n_2 = m = 2$.

$$\tilde{\mathbf{f}}_1(\mathbf{x}_1,\boldsymbol{\chi}_1,\mathbf{w}) = \begin{bmatrix} -a_1x_1+w_{11}S(\chi_1)+w_{14} \\ -a_2x_2+w_{21}S(\chi_2)+w_{22}S(\chi_1)S(\chi_3) \\ -a_3x_3+w_{31}S(\chi_3)+w_{32}S(\chi_1)S(\chi_2)\end{bmatrix}$$

$$\tilde{\mathbf{B}}_1(\mathbf{x}_1,\mathbf{w}) = \begin{bmatrix} -w_{12}S(\chi_3) & w_{13}S(\chi_2) \\ w_{23} & 0 \\ 0 & w_{33}\end{bmatrix}$$

For shorter notation all the weights are ordered in one vector $\mathbf{w} = \left[\mathbf{w}_1^\top \ \mathbf{w}_2^\top \ \mathbf{w}_3^\top\right]^\top$. This model can be reduced to the NBC-form [8], and therefore the block control methodology is applied. At first, the tracking error for neural output is rewritten as

$$\mathbf{z}_1 = \begin{bmatrix} z_1 \\ z_2\end{bmatrix} = \begin{bmatrix} x_1-\omega_r \\ \varphi-\varphi_r\end{bmatrix} \tag{6}$$

Then, the tracking error dynamics can be expressed as the first block of the NBC-form:

$$\dot{\mathbf{z}}_1 = \bar{\mathbf{f}}_1(\mathbf{x}_1,\boldsymbol{\chi}_1,\mathbf{w},\dot{\mathbf{y}}_r)+\bar{\mathbf{B}}_1(\boldsymbol{\chi}_1,\mathbf{w})\boldsymbol{\chi}_2 \tag{7}$$

where $\bar{\mathbf{B}}_1(\boldsymbol{\chi}_1,\mathbf{w}) = \begin{bmatrix} w_{12}S(\chi_3) & w_{13}S(\chi_2) \\ 2w_{23}\chi_2 & 2w_{33}\chi_3\end{bmatrix}$, $\bar{f}_{11} = -a_1x_1+w_{11}S(\chi_1)+w_{14}-\dot{\omega}_r$ and

$$\begin{aligned}\bar{f}_{12} &= 2x_2\left(-a_2x_2+\ w_{21}S(\chi_2)+w_{22}S(x_1)S(\chi_3)\right)+ \\ &\quad 2x_3(-a_3x_3+w_{31}S(\chi_3)+w_{32}S(\chi_1)S(\chi_2))-\dot{\varphi}_r\end{aligned}$$

Due to time variant nature of RHONN weights, we can not guarantee that rank($\bar{\mathbf{B}}_1$)= 2 for all time, so we assume that those parameters do not change their signs, keeping $\bar{\mathbf{B}}_1$ as a full rank matrix

To derive the control law, let start from equation (6), but with a slight change, which yields

$$\dot{\mathbf{z}}_1 = \bar{\mathbf{f}}_1(\mathbf{x}_1,\boldsymbol{\chi}_1,\mathbf{w},\dot{\mathbf{y}}_r)+\bar{\mathbf{B}}_1(\boldsymbol{\chi}_1,\mathbf{w})\boldsymbol{\chi}_1 = -\mathbf{K}\mathbf{z}_1+\mathbf{z}_2 \tag{8}$$

Solving the equation (8) for $\mathbf{z}_2$ results

$$\mathbf{z}_2 = \bar{\mathbf{f}}_1(\mathbf{x}_1,\boldsymbol{\chi}_1,\mathbf{w},\dot{\mathbf{y}}_r)+\bar{\mathbf{B}}_1(\boldsymbol{\chi}_1,\mathbf{w})\boldsymbol{\chi}_2+\mathbf{K}\mathbf{z}_1$$

Then the dynamics for $\mathbf{z}_2$ are

$$\dot{\mathbf{z}}_2 = \bar{\mathbf{f}}_2(\mathbf{x}_1,\boldsymbol{\chi},\mathbf{w},\mathbf{y}_r,\dot{\mathbf{y}}_r)+\bar{\mathbf{B}}_2(\boldsymbol{\chi}_1,\mathbf{w})\mathbf{u} \tag{9}$$

where $\bar{\mathbf{f}}_2(\mathbf{x}_1,\boldsymbol{\chi},\mathbf{w},\mathbf{y}_r,\dot{\mathbf{y}}_r) = \frac{\partial \mathbf{z}_2}{\partial \mathbf{x}_1}\tilde{\mathbf{f}}_1 + \frac{\partial \mathbf{z}_2}{\partial \boldsymbol{\chi}_1}\mathbf{f}_1 + \frac{\partial \mathbf{z}_2}{\partial \boldsymbol{\chi}_2}\mathbf{f}_2 + \frac{\partial \mathbf{z}_2}{\partial \mathbf{y}_r}\dot{\mathbf{y}}_r+\frac{\partial \mathbf{z}_2}{\partial \dot{\mathbf{y}}_r}\ddot{\mathbf{y}}_r + \frac{\partial \mathbf{z}_2}{\partial \mathbf{w}}\dot{\mathbf{w}}$ and $\bar{\mathbf{B}}_2(\boldsymbol{\chi}_1,\mathbf{w}) = \bar{\mathbf{B}}_1(\boldsymbol{\chi}_1,\mathbf{w})\mathbf{B}_2$.

Now, we select the desired sliding manifold as $\mathbf{z}_2 = \mathbf{0}$. The next scope is to design a control law that forces the system to reach the desired manifold. This controller must be a logic function which maps from the continuous state $\mathbf{x}$ to the admissible input vectors set U (see Table 1), in order to switch the control binary variables, such that, the desired voltage feeds the induction motor.

B. Sliding Modes Controller Design

Assumption 1. There exists at least one discrete value $\mathbf{u_k} \in U$, such that

$$\mathbf{sign}(\bar{\mathbf{B}}_2(\boldsymbol{\chi}_1,\mathbf{w})\mathbf{u_k}) = -\mathbf{sign}(\mathbf{z}_2), \text{for all } \mathbf{z}_2 \text{ with } \boldsymbol{\chi}_2,\boldsymbol{\chi}_3 \neq \mathbf{0} \tag{10}$$

The controller must select one element of U that satisfies (10), and then change the binary variables such that the selected input vector is fed to the stator windings. By using the model (1) instead of (3), the above assumption is proved in the Appendix (Section VIII).

Now we analyze the controller stability. Let $\bar{\mathbf{b}}_{21}$, $\bar{\mathbf{b}}_{22}$ the rows of $\bar{\mathbf{B}}_2(\boldsymbol{\chi}_1,\mathbf{w})$, then it can be expressed as

$$\bar{\mathbf{B}}_2(\boldsymbol{\chi}_1,\mathbf{w})\mathbf{u_k} == \begin{bmatrix} \left|\bar{\mathbf{b}}_{21}\mathbf{u_k}\right| & 0 \\ 0 & \left|\bar{\mathbf{b}}_{22}\mathbf{u_k}\right|\end{bmatrix}\begin{bmatrix} sign(\bar{\mathbf{b}}_{21}\mathbf{u_k}) \\ sign(\bar{\mathbf{b}}_{22}\mathbf{u_k})\end{bmatrix} \tag{11}$$

Using (10), the above expression can be formulated as

$$\begin{aligned}\bar{\mathbf{B}}_2(\boldsymbol{\chi}_1,\mathbf{w})\mathbf{u_k} &= \begin{bmatrix} \left|\bar{\mathbf{b}}_{21}\mathbf{u_k}\right| & 0 \\ 0 & \left|\bar{\mathbf{b}}_{22}\mathbf{u_k}\right|\end{bmatrix}\mathbf{sign}(\bar{\mathbf{B}}_2(\boldsymbol{\chi}_1,\mathbf{w})\mathbf{u_k}) \\ &= -\begin{bmatrix} \left|\bar{\mathbf{b}}_{21}\mathbf{u_k}\right| & 0 \\ 0 & \left|\bar{\mathbf{b}}_{22}\mathbf{u_k}\right|\end{bmatrix}\mathbf{sign}(\mathbf{z}_2)\end{aligned}$$

Hence, (9) is rewritten as

$$\dot{\mathbf{z}}_2 = \bar{\mathbf{f}}_2(\mathbf{x}_1,\boldsymbol{\chi},\mathbf{w},\mathbf{y}_r)-\mathbf{B}'(\boldsymbol{\chi}_1,\mathbf{w},\mathbf{u})\mathbf{sign}(\mathbf{z}_2) \tag{12}$$

where

$$\mathbf{B}'(\boldsymbol{\chi}_1,\mathbf{w},\mathbf{u}) = \begin{bmatrix} \left|\bar{\mathbf{b}}_{21}\mathbf{u_k}\right| & 0 \\ 0 & \left|\bar{\mathbf{b}}_{22}\mathbf{u_k}\right|\end{bmatrix}$$

Which guarantees a sliding mode on the surface $\mathbf{z}_2 = \mathbf{0}$ at some finite time. under the condition

$$\left|\bar{f}_{21}\right| < \left|\bar{\mathbf{b}}_{21}\mathbf{u_k}\right| \text{ and } \left|\bar{f}_{22}\right| < \left|\bar{\mathbf{b}}_{21}\mathbf{u_k}\right| \tag{13}$$

Then the sliding dynamics, in the tracking errors variables z_1 and z_2 (6), is governed by the second order linear system

$$\begin{aligned}\dot{z}_1 &= -k_1z_1 \\ \dot{z}_2 &= -k_2z_2\end{aligned}$$

with desired eigenvalues $-k_1$ and $-k_2$.

Note that some of the available input vectors, presented in Table 1 may satisfy the condition (10), at the same time; we select the input vector that maximizes $\left\|\bar{\mathbf{B}}_2(\boldsymbol{\chi}^1,\mathbf{w})\mathbf{u_k}\right\|$, in order to increase the sliding motion stability margin given by (13).

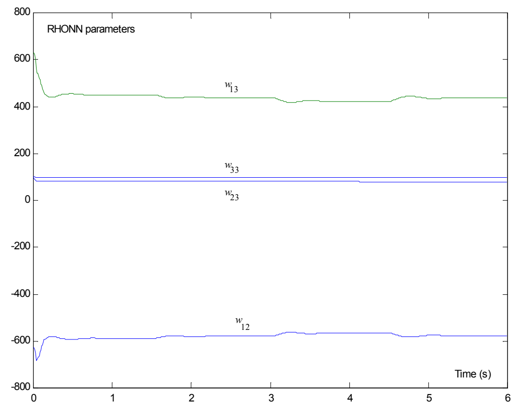

Fig. 4. Weigths w_{12}, w_{13}, w_{23} and w_{33}.

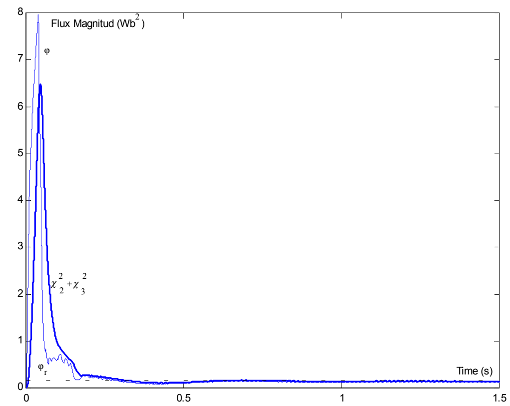

Fig. 6. Motor flux magitud $\chi_2^2 + \chi_3^2$, neural flux magnitude φ and its reference φ_r

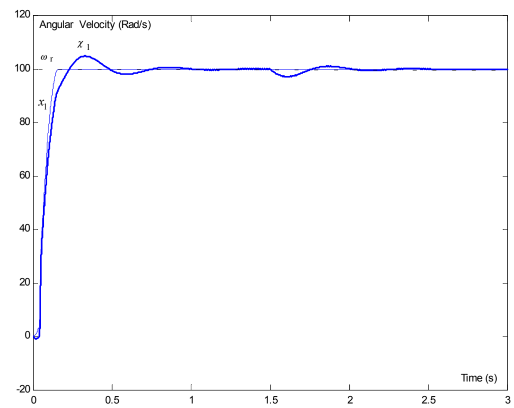

Fig. 5. Motor velocity χ_1, and RHONN velocity x_1 and its reference ω_r.

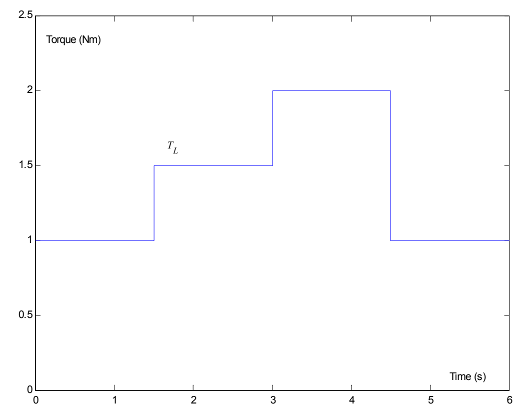

Fig. 7. Load torque T_L

VI. Simulation Results

We simulate the proposed control scheme using Simulink Matlab®. The nominal values of the induction motor parameters are: $R_s = 12.53\Omega$, $L_s = 0.2464H$, $M = 0.2219H$, $R_r = 11.16\Omega$, $L_r = 0.2464H$, $n_p = 2$, $J = 0.01Kgm$, The design parameters for the fluxes observer are $l_1, l_2 = 3500$ and $\delta = 0.1$; for the neural network, we selected $a_1 = 18$, $a_2 = a_3 = 500$, $\beta = 0.1$, $\Gamma_1^{-1} = diag\{200, 200, 200\}$, $\Gamma_2^{-1} = \Gamma_3^{-1} = diag\{500, 500, 50\}$, and $k_1 = 160$ $k_2 = 140$, $\omega_r = 100Rad/s$ and $\varphi_r = 0.15$.

In order to test the proposed scheme performance, a variation of 2 Ohm per second is added to the stator resistance, in addition the load torque is a switching signal, see Fig.7.

The results for velocity and flux are presented in Fig. 5 and Fig. 6, respectively. As can be seen, the performance of the proposed scheme is very satisfactory under disturbances.

VII. Conclusions and Future Work

In this paper, we have proposed a VSC methodology, for induction motors, which guarantees asymptotic stability under one of the hardest technological constraints, the switching nature of the electrical drivers. This control scheme let us to avoid the PWM approach, and gives us an actuator model closer to the real one. The stability, for both the neural identifier and the controller, is analyzed, and it is proved that the proposed control law forces the closed loop trajectory to converge and to stay in a manifold, which guarantees that the tracking error is zero. The robustness of this control scheme is tested in presence of different kind of disturbances such as load torque variations and change on the induction motor parameters.

Acknowledgments — The authors thank the support of CONACYT, Mexico, on Project 36960A.

VIII. Appendix

Suppose that we are control law in based on model (1) insted of (3). Following the block control technique until equation (9), then the term $\bar{\mathbf{B}}_2(\mathbf{x}_1)\mathbf{u}$ describes a $\mathbf{x}_1-$dependent bilinear transformation, which maps from the discrete input space U to the continuous space, or

$\bar{\mathbf{B}}_\mathbf{2}(\mathbf{x_1})\mathbf{u} : \mathbf{U} \rightarrow \Re^\mathbf{2}$. Because the matrix $\bar{\mathbf{B}}_\mathbf{2}(\mathbf{x_1})$ has full rank for all $\psi_\alpha, \psi_\beta \neq 0$, it maps from two different elements of U onto different vectors in $\Re^2$. Now, we rewrite

$$\bar{\mathbf{B}}_\mathbf{2} = \mathbf{B}_\mathbf{2}'\mathbf{B_0}$$

where $\mathbf{B}_\mathbf{2}' = \begin{bmatrix} c_1c_7 & 0 \\ 0 & 2c_3c_7 \end{bmatrix}$, $\mathbf{B_0} = \begin{bmatrix} -\boldsymbol{\chi}_\mathbf{3} & \boldsymbol{\chi}_\mathbf{2} \\ \boldsymbol{\chi}_\mathbf{2} & \boldsymbol{\chi}_\mathbf{3} \end{bmatrix}$

Hence, the mapping $\bar{\mathbf{B}}_\mathbf{2}$ can be seen as a composition of two transformations defined by $\mathbf{B_0}$ and $\mathbf{B}_\mathbf{2}'$.

In order to have a simple terminology, we establish the following definition:

Definition 2: A 2-by-1 vector set covers all the quadrants in $\Re^2$ space, if at least one of them lies on each one of the space quadrants.

As can be seen in Fig. 2, U covers all the quadrants of the input space. Let V be the image of the set U under the mapping $\mathbf{B_0}$. By the following lemma we can assure that V also covers all the quadrants.

Lemma 3: The angle between any pair of vectors of U is equal to the one between their corresponding images under the mapping B_0.

Proof: $\mathbf{B_0}$ is a symmetric type matrix, whose columns $\mathbf{b_{01}}$ and $\mathbf{b_{02}}$ are orthogonal and $\mathbf{b_{01}^\top b_{01}} = \mathbf{b_{02}^\top b_{02}} = \varphi$. It follows that $\mathbf{B_0^\top B_0} = \varphi\mathbf{I}$, hence $\|\mathbf{B_0 u}\| = \sqrt{\mathbf{u^\top B_0^\top B_0 u}} = \sqrt{\varphi}\,\|\mathbf{u}\|$. Let $\mathbf{u_i}$ and $\mathbf{u_j}$ be two different elements in U. By the Euclidean inner product, we have

$$\mathbf{u_i}^\top \mathbf{u_j} = \|\mathbf{u_i}\|\,\|\mathbf{u_j}\|\cos(\boldsymbol{\theta})$$

where θ is the angle between the vectors. Let $\mathbf{v_i},\mathbf{v_j} \in V$ be the images of $\mathbf{u_j}$ and $\mathbf{u_j}$, respectively, then

$$\mathbf{v_i}^\top \mathbf{v_j} = \|\mathbf{v_i}\|\,\|\mathbf{v_j}\|\cos(\boldsymbol{\theta}') \tag{14}$$

with θ' the angle between $\mathbf{v_i}$ and $\mathbf{v_j}$. Now substituting $\mathbf{v} = \mathbf{B_0 u}$ in (14) we obtain

$$\mathbf{u_i}^\top \mathbf{B_0^\top B_0 u_j} = \varphi \mathbf{u_i}^\top \mathbf{u_j} = \boldsymbol{\varphi}\,\|\mathbf{u_i}\|\,\|\mathbf{u_j}\|\cos(\boldsymbol{\theta}')$$

then $\cos(\theta') = \cos(\theta)$, and the proof is completed. ■

The following lemma states the sliding mode controller viability, using only the available input vectors given by the Table 1.

Lemma 4: There exists at least one available input vector $\mathbf{u_k} \in U$, such that

$$\mathbf{sign}(\bar{\mathbf{B}}_\mathbf{2}\mathbf{u_k}) = -\mathbf{sign}(\mathbf{z_2}), \textit{for all } \mathbf{z_2} \textit{ and } \boldsymbol{\psi_\alpha}, \boldsymbol{\psi_\beta} \neq \mathbf{0} \tag{15}$$

Proof: This lemma statement is equivalent to say that the images of U under $\bar{\mathbf{B}}_\mathbf{2}$ covers all the quadrants. From Lemma 3, it follows that V covers all the quadrants. Now let W be the image of V under $\mathbf{B}_\mathbf{2}'$. It is clear that this mapping just changes the axes scale. Hence, it does not move any vector from its original quadrant, hence W covers all the quadrants too. Then, we can conclude that there exists, at least, one image of the elements of U under $\bar{\mathbf{B}}_\mathbf{2}$ on each quadrant of $\Re^2$. Hence, there is one or more available input vectors that satisfies (15). ■

References

[1] K. Bose, *Power Electronics and AC Drives*, Prentice Hall, New Jersey, U.S.A.1986.

[2] G. Buja, D. Casadei and G. Serra "Direct stator flux and torque control of a induction motor: theoretical and experimental results". Proc. IEEE-IECON, pages T50-T64, Aachen Germany, 1998.

[3] M. Depenbrock. "Direct self Control of inverter-fed induction machines" IEEE Trans. Power Electr., Vol. 3, pp. 420-429, 1998

[4] M. M. Gupta and D. H. Rao (Eds.), *Neuro-Control Systems, Theory and Applications*, IEEE Press.

[5] P. A. Ioannou and J. Sun. *Robust Adaptive Control*, Prentice Hall, New Jersey, USA. 1996.

[6] E. B. Kosmatopoulus, M. M. Polycarpou, M. A. Christodolou and P. A. Ioannou "High order neural network structures for identification of dynamical systems", *IEEE Transactions on Neural Networks*, vol. 6, pp. 422-431, 1995

[7] W. Leonhard *Control of Electrical Drivers*, Springer, 1996

[8] A. G. Loukianov. "Nonlinear block control with sliding mode", *Automation and Remote Control*, Vol.59, No.7, pp. 916-933. 1998.

[9] A.G. Loukianov, E. N. Sanchez and R.A. Felix "Induction Motor VSC Control Using Neural Networks", 15th IFAC World Congress, Barcelona, Spain, July 2002.

[10] A. D. Luca and G. Ulivi, "Design of exact nonlinear controller for induction motors", *IEEE Trans. Automat. Control*, Vol.34, pp. 1304-1307, 1989.

[11] R. Ortega, N. Barabanov, G. Escobar "Direct Torque Control of Induction Motors: Stability Analysis and Performance Improvement" *IEEE Trans. Aut. Control*, Vol. 46, No. 8, Aug 2001, pp. 1209–1222.

[12] A. S. Poznyak, W. Yu, E. N. Sanchez, and J. P. Perez, "Nonlinear adaptive trajectory tracking using dynamic neural networks", *IEEE Trans. on Neural Networks*, vol. 10, No 6, pp 1402-1411, Nov. 1999.

[13] G. A. Rovithakis and M. A. Christodolou. "Adaptive control of unknown plants using dynamical neural networks", *IEEE Transactions on Systems, Man and Cybernetics*, vol. 24, pp 400-412. 1994.

[14] E. N. Sanchez, A. G. Loukianov, R. A. Felix "Stepper Motor Trajectory Tracking via Dynamic Triangular Neural Networks". 15th IEEE International Symposium on Intelligent Control ISIC 2000. University of Patras Greece. July 2000.

[15] E. N. Sanchez, A. G. Loukianov, R. A. Felix "Recurrent Neural Block Form Control" *Automatica*, No. 39, pp. 1275-1282. 2003

[16] V. I. Utkin, *Sliding Modes in Control and Optimization*, Springer Verlag, New York, 1992.